

Stimulated Raman amplification and lasing in silicon photonic band gap nanocavities

Xiaodong Yang*, Chee Wei Wong

Optical Nanostructures Laboratory, Columbia University, New York, NY 10027, USA

Received 8 July 2005; received in revised form 10 January 2006; accepted 7 March 2006

Available online 24 July 2006

Abstract

The concept and design of L5 photonic band gap nanocavities in two-dimensional (2D) photonic crystal (PhCs) slabs for enhancement of stimulated Raman amplification and lasing in monolithic silicon is suggested for the first time. Specific high quality factor (Q) and small modal volume nanocavities are designed which supports the required pump–Stokes modal spacing in silicon, with ultra-low lasing thresholds.

© 2006 Elsevier B.V. All rights reserved.

Keywords: Stimulated Raman scattering; Lasing; Photonic band gap nanocavity; Silicon photonics

1. Introduction

Photonic crystals (PhCs) are periodic dielectric structures that have a band gap that forbids propagation of a certain frequency range of light [1]. Silicon is increasingly being considered as a dominant platform for photonic integrated circuits, which can be integrated with CMOS-compatible silicon electronics [2]. Two-dimensional (2D) PhC slabs are widely used for optical applications nowadays. With high- Q/V_m nanocavities [3–5] designed by k -space engineering of the cavity modes [6], light confinement and also light-matter interaction are enhanced so that both the device size and the energy consumption can be significantly reduced. These high- Q/V_m nanocavities have critical importance in fundamental studies and integrated nanophotonics applications, such as channel add/drop filters [7], quantum well lasers [8], cavity quantum electrodynamics [9], enhancement of optical nonlinearities [10], and ultrasmall nonlinear bistable devices [11].

For the enhancement of stimulated Raman scattering (SRS) in high- Q microcavity, recent work in silica-based designs have shown remarkable ultra-low threshold microcavity Raman lasers in silica microspheres [12] and silica microdisks [13] with excited whispering gallery modes. The bulk Raman gain coef-

ficient g_R in silicon is 10^3 – 10^4 times higher than in silica. Light generation and amplification in planar silicon waveguides with Raman effects are studied recently [14–18]. Raman lasing using a silicon waveguide as the gain medium was also demonstrated [19–23]. Two-photon absorption (TPA) induced free-carrier absorption (FCA) [24] is addressed using pulsed operation or reversed biased p-i-n diodes. Here we suggest, for the first time, the enhanced stimulated Raman amplification and low-threshold Raman lasing that can be achieved with high- Q/V_m photonic band gap nanocavities in 2D PhC slabs [25]. This permits applications such as wavelength-selectable signal amplification and lasing in monolithic silicon for photonic integrated circuits, novel microlasers at new wavelengths, and facilitate and further advance the study of nonlinear phenomena at small lengthscales. As a specific example, we illustrate the concept and the design of enhanced stimulated Raman amplification and lasing in a L5 photonic band gap nanocavity, with which low lasing thresholds on order of tens to hundreds of μW are predicted.

2. Design concept and theoretical background

Stimulated Raman scattering is a two-photon process related to the optical phonons. The strongest Stokes peak arises from single first-order Raman phonon (three-fold degenerate) at the Brillouin zone center. Coupling between the pump and Stokes waves in SRS can be understood classically with nonlinear polarizations $P^{(3)}$, where $P^{(3)}$ is $\chi_{ikmn}^{(3)} E_p E_p^* E_s$, $\chi_{ikmn}^{(3)}$ the third-order

* Corresponding author. Tel.: +1 212 854 7253; fax: +1 212 854 3304.

E-mail addresses: xy2103@columbia.edu (X. Yang),
cww2104@columbia.edu (C.W. Wong).

fourth-rank Raman susceptibility, and E_p and E_s are the electric fields of the pump and Stokes waves, respectively. The dynamics of SRS is governed through a set of time-dependent coupled nonlinear equations [26]. Here, we employ the usual slowly varying envelope approximation for the forward and backward propagation pump wave amplitudes A_p^\pm and Stokes wave amplitudes A_s^\pm . The coupled nonlinear equations are described by [27–29]:

$$\begin{aligned} \pm \frac{\partial A_p^\pm}{\partial z} + \frac{1}{v_p} \frac{\partial A_p^\pm}{\partial t} = & \left\{ -\frac{g_p}{2} (|A_s^+|^2 + |A_s^-|^2) + i\gamma_p [|A_p^\pm|^2] \right. \\ & + 2(|A_p^\mp|^2 + |A_s^+|^2 + |A_s^-|^2) - \frac{\alpha_p}{2} - \beta [|A_p^\pm|^2 + 2(|A_p^\mp|^2 \\ & \left. + |A_s^+|^2 + |A_s^-|^2)] - \bar{\varphi} \lambda_p^2 \bar{N}_{\text{eff}} \right\} A_p^\pm \end{aligned} \quad (1)$$

$$\begin{aligned} \pm \frac{\partial A_s^\pm}{\partial z} + \frac{1}{v_s} \frac{\partial A_s^\pm}{\partial t} = & \left\{ \frac{g_s}{2} (|A_p^+|^2 + |A_p^-|^2) + i\gamma_s [|A_s^\pm|^2] \right. \\ & + 2(|A_s^\mp|^2 + |A_p^+|^2 + |A_p^-|^2) - \frac{\alpha_s}{2} - \beta [|A_s^\pm|^2 + 2(|A_s^\mp|^2 \\ & \left. + |A_p^+|^2 + |A_p^-|^2)] - \bar{\varphi} \lambda_s^2 \bar{N}_{\text{eff}} \right\} A_s^\pm + i\kappa A_s^\mp + i\delta\beta A_s^\pm \end{aligned} \quad (2)$$

Here, material dispersion is considered negligible compared to the cavity dispersion, and only the first-order Stokes is considered. The first two terms on the right-hand side represent SRS and Kerr nonlinearities, respectively, with $g_{p,s}$ the Raman gain coefficients (20–76 cm/GW in silicon have been reported [28] in the 1550-nm range) for the pump and Stokes waves and $\gamma_{p,s}$ the Kerr nonlinear coefficients ($=2\pi n_2/\lambda_{p,s}$). In the Kerr term, the $2|A_j|^2 A_k$ terms represent cross-phase modulation, while the $|A_j|^2 A_k$ terms represent self-phase modulation. $v_{p,s}$ are group velocities. The α -terms account for linear loss, the κ -terms account for forward and backward coupling, and the $\delta\beta$ -terms account for signal detuning from Bragg resonance. The constant β is the two-photon absorption coefficient of silicon, $\bar{\varphi}$ is related to the efficiency of the free-carrier absorption process, and \bar{N}_{eff} is the effective charge-carrier density. The above-coupled equations can be employed for cw or pulsed signals and pumps. The effective $A_{p,s}^\pm$ can be calculated inside high- Q/V_m nanocavities together with the Fabry–Perot model [30].

Classical field accumulation of both $|A_s|^2$ and $|A_p|^2$ intensities (seen in Eqs. (1) and (2)) within a cavity enhances the spontaneous and stimulated Raman scattering process, since the Raman gain coefficient is intensity-dependent. For laser oscillation, the gain condition requires the round-trip gain G_R to exceed the round-trip loss α for initiation of oscillation: $(G_R - \alpha) > 0$. The power build up in a cavity has a Q/V_m dependence, while the cavity round-trip loss has a $1/Q$ dependence from the definition of Q . Equating G_R with α , the lasing threshold $P_{\text{threshold}}$ can be described by:

$$P_{\text{threshold}} = \frac{\pi^2 n_s n_p}{g_s \xi \lambda_s \lambda_p} \frac{V_m}{Q_s Q_p} \quad (3)$$

where V_m is the effective modal volume, ξ the modal overlap, $Q_{p,s}$ the cavity quality factors, $n_{p,s}$ the refractive indices at the pump and Stokes wavelengths λ_p and λ_s , respectively. Both the

pump and Stokes in the nanocavity are designed to have the same (e.g. even) symmetry to maximize the overlap ξ between the modes. The character of this threshold is similar to that derived for whispering gallery modes in microspheres and microcavities [12,13]. Note that the bulk Raman gain $g_s = g_b$ above is still in the classical formulation, without considerations of possible cavity quantum electro-dynamics (QED) enhancements.

The lasing threshold scales with $V_m/Q_s Q_p$ as illustrated in Eq. (3). This, therefore, suggests the motivation for small V_m cavities with high- Q factors. In fact, for microscopic spherical cavities (with $\sim 70 \mu\text{m}$ radius) where V_m has an approximate quadratic dependence on the lengthscale L , a L^2 dependence for the Raman lasing threshold has been observed experimentally [12]. For even smaller spherical microdroplets, with $4 \mu\text{m}$ radius, a stronger L^4 dependence has been observed experimentally on the Raman lasing threshold [31]. This additional L^2 dependence in the microdroplets is attributed to cavity QED enhancements, particularly when the cavity linewidths are significantly smaller than the homogenous linewidth of the scattering process (when Fermi's golden rule breaks down). Here, the Raman gain in the cavity $g_s = g_c$ is approximated by the density of states with the cavity compared to the free space density [32,33] and the transition rate per mode, although there are also counter opinions that cavity QED enhancement is not significant [34]. Even without the cavity QED enhancements and considering only classical local field enhancement, the Raman lasing threshold in silicon photonic band gap nanocavities is estimated on order tens to hundreds of μW . This estimate is based on the high- Q/V_m nanocavities designed in following section.

Analysis of the possible cavity enhancement of the Raman gain coefficient g_c is explored by several groups [12,31,35,36]. For example, Wu et al. [36] and Lin et al. [31] have discussed cavity enhancement, either through a three-level atom-cavity Λ configuration or an estimate directly from the density of states in the cavity, respectively. The resulting enhancements have a $1/L^2$ or $1/L$ dependence [37]. For the designed nanocavities (discussed in following section), the cavity-enhanced gain coefficient is estimated on order 10^2 larger than the bulk gain coefficient. An alternative approach would be to use an effective SRS path length interaction method, such as in Lin et al. [31] and Matsko et al. [34], as a first-order approximation to the Raman gain of the Stokes signal ($\sim \exp(g_c I_c L_c)$), where I_c is the intensity of pump light stored in the cavity, and the effective interaction length L_c is described as: $L_c = Q\lambda/2\pi n$. For example, the high- Q subwavelength nanocavity described in the next section has an effective interaction length on order 3 mm, a factor of 1.2×10^3 larger than the physical cavity length ($\sim 2.5 \mu\text{m}$) for a cavity Q of 4.2×10^4 .

The next section focuses on the numerical design of specific photonic band gap nanocavities to support Raman amplification and lasing in monolithic silicon.

3. Design and analysis

We consider here a specific photonic band gap nanocavity with linearly aligned missing air holes. The nanocavity is designed numerically with MIT Photonic Bands (MPB) package

Table 1
Design summary of photonic crystal L5 nanocavity for Raman lasing in silicon

S_1 ($\times a$)	a (nm)	λ_{pump} (nm)	Q_{pump}	λ_{Stokes} (nm)	Q_{Stokes}
0	456	1592	560	1735.6	20693
0.05	414	1456.4	739	1575.8	19036
0.07	395	1395.7	863	1505	20843
0.10	376	1333.1	1030	1432.4	24642
0.15	342	1215.2	1550	1297.1	42445

[38] and 3D FDTD method [39]. Using MPB, the photonic band structure and the resonant frequencies can be obtained. With 3D FDTD method, the resonant wavelength, field profiles and Q can be calculated. The goal of the design is to tune the frequencies of pump mode (f_{pump}) and Stokes mode (f_{Stokes}) with spacing 15.6 THz, corresponding to the optical phonon frequency in monolithic silicon. The wavelengths are also tuned to operate around 1550 nm, with high Q_s (on order 10,000 or more) for at least the Stokes mode. The numerical design process is as following: (1) fine-tune the cavity geometry; (2) calculate resonant frequencies f_{pump} and f_{Stokes} with MPB; (3) calculate the lattice constant a based on the frequencies ($f_{\text{pump}} - f_{\text{Stokes}})(c/a) = 15.6$ THz and calculate the wavelength $\lambda_{\text{pump}} = a/f_{\text{pump}}$, $\lambda_{\text{Stokes}} = a/f_{\text{Stokes}}$; (4) Calculate Q_{pump} and Q_{Stokes} with 3D FDTD method. The same process can be used to design nanocavities for anti-Stokes cavity-enhancement, where anti-Stokes generation typically has appreciably lower scattering magnitudes.

The structure investigated is an air-bridge triangular lattice photonic crystal slab with thickness of $0.6a$ and the radius of air holes is $0.29a$, where a is the lattice period. The photonic band gap in this slab for TE-like modes is around $0.25\text{--}0.32$ [c/a] in frequency. Two even modes supported in L3, L4, L5 cavities with linearly aligned missing air holes are studied, with which the modal overlap will be maximized. For small cavities such as L3 and L4, calculated a and λ are large, which will not match the telecommunication applications (around 1550 nm wavelength). For example, in L3 cavity, $S_1 = 0.15a$, $a = 685$ nm, $\lambda_{\text{pump}} = 2266$ nm and $\lambda_{\text{Stokes}} = 2568$ nm. Finally, two even modes in single L5 cavity are used as pump mode and Stokes mode for Raman lasing, respectively. Fig. 1(a) shows the two modal resonant peaks when a Gaussian impulse is launched in the center of L5 cavity.

Table 1 gives the design summary of fine-tuning the shift S_1 of two air-holes at cavity edge. When increasing S_1 , the calculated lattice period a decreases and the resonant wavelength λ also decreases due to the constant optical phonon frequency. The quality factors increase because the electric field profile is close to Gaussian function and has less leakage. The bold values in Table 1 highlight the desired design parameters. Fig. 1(b) compares the quality factor of pump mode and Stokes mode for different shift of two air holes $S_1 = 0\text{--}0.15a$. Q values are obtained by calculating modal transient energy decay with 3D FDTD method: $Q = \omega_0 U/P = -\omega_0 U/(dU/dt)$, where U is the stored energy, ω_0 the resonant frequency, and $P = -(dU/dt)$ is the power dissipated. Q_{pump} and Q_{Stokes} are in the order of 10^3 and 10^5 , respectively. Higher- Q nanocavities can be achieved by fine-tuning the shift of additional air-holes at cavity edge

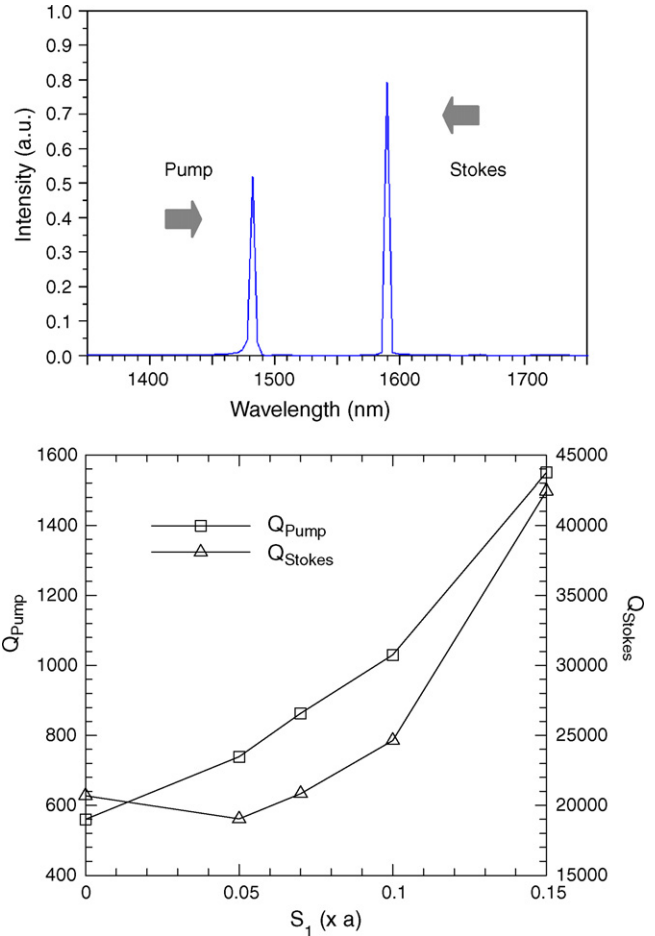


Fig. 1. (a) Resonant peak of pump and Stokes modes within photonic band gap and (b) Q_{pump} and Q_{Stokes} as a function of shift S_1 .

such as S_2 and S_3 without changing the effective modal volume [3]. Using the ultra-high- Q photonic double-heterostructure nanocavities is also possible [5]. The designed wavelength of Stokes mode is around 1550 nm and the L5 cavity with $S_1 = 0.05a$ and $a = 414$ nm is considered in the following calculation.

Figs. 2 and 3 show the electric field profile (E_y) and 2D Fourier transform (FT) spectrum of E_y at the middle of the slab for pump mode and Stokes mode, respectively, where the shift S_1 of air holes is $0.05a$. Both modes are of even symmetry to maximize the modal overlap. Currently, the modal overlap is around 0.1 between pump mode and Stokes mode due to the small cavity size and the discrete distribution of air holes in PhC slabs. The white circle is the boundary of the light cone. There is a trade-off between the wavelength λ and the quality factor Q . For

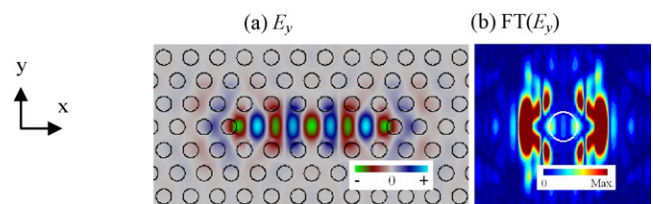


Fig. 2. The electric field profile (E_y) (a) and 2D FT spectrum (b) of pump mode.

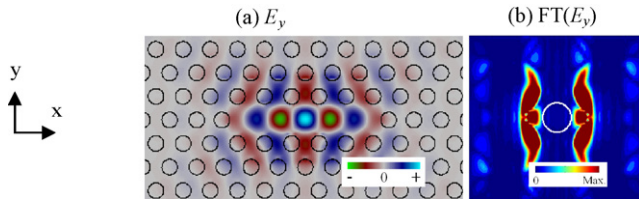


Fig. 3. The electric field profile (E_y) (a) and 2D FT spectrum (b) of Stokes mode.

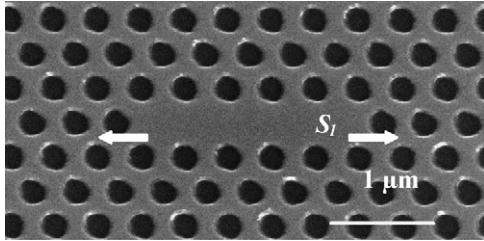


Fig. 4. SEM picture of the PhC L5 nanocavity for Raman lasing in silicon.

example, Q is highest for $S_1 = 0.15a$, but the wavelengths are far from 1550 nm. In Fig. 2(b), the FT spectrum of the pump mode contains large components inside the light cone, which indicates the lower Q , whereas the FT spectrum of Stokes mode contains much smaller components inside it and corresponds to high Q , which is shown in Fig. 3(b). The higher order mode (pump mode here) has the more serious edge effect, then decreasing Q . Fig. 4 shows the scanning electron microscopy (SEM) of the fabricated L5 nanocavity in 2D PhC slab for Raman amplification and lasing in silicon.

The estimated modal volume for L5 cavity is around $10.56(\lambda/2n)^3$ from ref. [40], which is $V_m \sim 0.12 \mu\text{m}^3$. The Raman lasing threshold $P_{\text{threshold}}$ in L5 nanocavity estimated from Eq. (3) is around $130 \mu\text{W}$ based on parameters $g_s = 70 \text{ cm/GW}$, $\xi = 1$, $\lambda_{s,p} = 1550 \text{ nm}$, $Q_{\text{pump}} = 1550$ and $Q_{\text{Stokes}} = 4.2 \times 10^4$. With higher- Q nanocavities, the threshold can go down on order several to tens of μW . In comparison with silica-based ultra-high- Q microspheres, the lower Q in photonic band gap nanocavities is compensated by the 10^3 – 10^4 larger bulk Raman gain in silicon compared to silica, and the significantly smaller modal volume of the silicon nanocavities. This motivates the approach towards employing ultrasmall photonic band gap nanocavities with high- Q factors for ultralow threshold Raman lasers in monolithic silicon.

4. Conclusion

The concept and design of L5 photonic band gap nanocavities in two-dimensional photonic crystal slabs for enhancement of stimulated Raman amplification and lasing in monolithic silicon is presented for the first time. Specifically, we describe the numerical design of a high quality factor and small modal volume nanocavity that supports the required pump–Stokes modal spacing in silicon, with ultralow lasing thresholds, which supports the ultimate push towards all-optical signal amplification and lasing in on-chip monolithic silicon.

Acknowledgment

This work is supported by the Columbia Initiative in Science and Engineering for Nanophotonics.

References

- [1] J.D. Joannopoulos, et al., *Photonic Crystals: Molding the Flow of Light*, Princeton University Press, Princeton, 1995;
- E. Yablonovitch, Inhibited spontaneous emission in solid-state physics and electronics, *Phys. Rev. Lett.* 58 (1987) 2059;
- S. John, Strong localization of photons in certain disordered dielectric superlattices, *Phys. Rev. Lett.* 58 (1987) 2486.
- [2] L. Pavesi, D.J. Lockwood, *Silicon Photonics*, Springer-Verlag, New York, 2004.
- [3] Y. Akahane, et al., High- Q photonic nanocavity in a two-dimensional photonic crystal, *Nature* 425 (2003) 944–947.
- [4] Y. Akahane, T. Asano, B. Song, S. Noda, Fine-tuned high- Q photonic-crystal nanocavity, *Opt. Express* 13 (2005) 1202–1214.
- [5] B.S. Song, et al., Ultra-high- Q photonic double-heterostructure nanocavity, *Nat. Mater.* 4 (2005) 207–210.
- [6] K. Srinivasan, O. Painter, Momentum space design of high- Q photonic crystal optical cavities, *Opt. Express* 10 (2002) 670–684.
- [7] Y. Akahane, T. Asano, H. Takano, B. Song, Y. Takana, S. Noda, Two-dimensional photonic-crystal-slab channel-drop filter with flat-top response, *Opt. Express* 13 (2005) 2512–2530.
- [8] Y.H. Lee, et al., Electrically driven single-cell photonic crystal laser, *Science* 305 (2004) 1444.
- [9] D.G. Deppe, et al., Vacuum Rabi splitting with a single quantum dot in a photonic crystal nanocavity, *Nature* 432 (2004) 200.
- [10] M. Soljacic, J.D. Joannopoulos, Enhancement of nonlinear effects using photonic crystals, *Nat. Mater.* 3 (2004) 211–219.
- [11] M. Notomi, A. Shinya, S. Mitsugi, G. Kira, E. Kuramochi, T. Tanabe, Optical bistable switching action of Si high- Q photonic-crystal nanocavities, *Opt. Express* 13 (2005) 2678–2687.
- [12] M. Spillane, T.J. Kippenberg, K.J. Vahala, Ultralow-threshold Raman laser using a spherical dielectric microcavity, *Nature* 415 (2002) 621–623.
- [13] T.J. Kippenberg, S.M. Spillane, D.K. Armani, K.J. Vahala, Ultralow-threshold microcavity Raman laser on a microelectronic chip, *Opt. Lett.* 29 (2004) 1224–1226.
- [14] R. Claps, et al., Observation of Raman emission in silicon waveguides at $1.54 \mu\text{m}$, *Opt. Express* 10 (2002) 1305–1313;
- R. Claps, et al., Observation of stimulated Raman amplification in silicon waveguides, *Opt. Express* 11 (2003) 1731–1739;
- R. Claps, et al., Anti-Stokes Raman conversion in silicon waveguides, *Opt. Express* 11 (2003) 2862–2872.
- [15] R.L. Espinola, et al., Raman amplification in ultrasmall silicon-on-insulator wire waveguides, *Opt. Express* 12 (2004) 3713–3718.
- [16] Q. Xu, et al., Time-resolved study of Raman gain in highly confined silicon-on-insulator waveguides, *Opt. Express* 12 (2004) 4437–4442.
- [17] T.K. Liang, H.K. Tsang, Efficient Raman amplification in silicon-on-insulator waveguides, *Appl. Phys. Lett.* 85 (2004) 3343–3345.
- [18] A. Liu, et al., Net optical gain in a low loss silicon-on-insulator waveguide by stimulated Raman scattering, *Opt. Express* 12 (2004) 4261–4268.
- [19] O. Boyraz, B. Jalali, Demonstration of a silicon Raman laser, *Opt. Express* 12 (2004) 5269–5273.
- [20] R. Jones, et al., Net continuous wave optical gain in a low loss silicon-on-insulator waveguide by stimulated Raman scattering, *Opt. Express* 13 (2005) 519–525.
- [21] H. Rong, et al., An all-silicon Raman laser, *Nature* 433 (2005) 292–294;
- H. Rong, et al., A continuous-wave Raman silicon laser, *Nature* 433 (2005) 725–728.
- [22] O. Boyraz, B. Jalali, Demonstration of directly modulated silicon Raman laser, *Opt. Express* 13 (2005) 796–800.
- [23] R. Jones, et al., Lossless optical modulation in a silicon waveguide using stimulated Raman scattering, *Opt. Express* 13 (2005) 1716–1723.

- [24] H.K. Tsang, et al., Optical dispersion, two-photon absorption and self-phase modulation in silicon waveguides at 1.5 μm wavelength, *Appl. Phys. Lett.* 80 (2002) 416–418.
- [25] X. Yang, J. Yan, C.W. Wong, Design and fabrication of L5 photonic band gap nanocavities for stimulated Raman amplification in monolithic silicon *CLEO/QELS*, Baltimore, Maryland, May 2005, 2005.
- [26] Y.R. Shen, *The Principles of Nonlinear Optics*, Wiley, Hoboken, New Jersey, 2003.
- [27] V.E. Perlin, H.G. Winful, Stimulated Raman scattering in nonlinear periodic structures, *Phys. Rev. A* 64 (2001) 043804.
- [28] M. Krause, H. Renner, E. Brinkmeyer, Analysis of Raman lasing characteristics in silicon-on-insulator waveguides, *Opt. Express* 12 (2004) 5703–5710.
- [29] R.G. Zaporozhchenko, et al., Stimulated Raman scattering of light in a photonic crystal, *Quan. Elect.* 30 (2000) 997–1001.
- [30] C. Sauvan, P. Lalanne, J.P. Hugonin, Slow-wave effect and mode-profile matching in photonic crystal microcavities, *Phys. Rev. B* 71 (2005) 165118.
- [31] H.-B. Lin, A.J. Campillo, cw Nonlinear optics in droplet microcavities displaying enhanced gain, *Phys. Rev. Lett.* 73 (1994) 2440; H.-B. Lin, A.J. Campillo, Microcavity enhanced Raman gain, *Opt. Commun.* 133 (1997) 287.
- [32] H. Yokoyama, S.D. Brorson, Rate equation analysis of microcavity lasers, *J. Appl. Phys.* 66 (1989) 4801.
- [33] H.M. Lai, P.T. Leung, K. Young, Electromagnetic decay into a narrow resonance in an optical cavity, *Phys. Rev. A* 37 (1988) 1597.
- [34] A.B. Matsko, A.A. Savchenkov, R.J. Letargat, V.S. Ilchenko, L. Maleki, On cavity modification of stimulated Raman scattering, *J. Opt. B: Quantum Semiclass. Opt.* 5 (2003) 272–278.
- [35] B. Min, T.J. Kippenberg, K.J. Vahala, Compact, fiber-compatible, cascaded Raman laser, *Opt. Lett.* 28 (2003) 1507.
- [36] Y. Wu, X. Yang, P.T. Leung, Theory of microcavity-enhanced Raman gain, *Opt. Lett.* 24 (1999) 345; Y. Wu, P.T. Leung, Lasing threshold for whispering-gallery-mode microsphere lasers, *Phys. Rev. A* 60 (1999) 630.
- [37] For a one-dimensional cavity, the enhancement reduces to the Yokoyama-Brorson factor (Yokoyama and Brorson, *J. Appl. Phys.* 66 (1989) 4801) as suggested in Wu et al. *Opt. Lett.* 24 (1999) 345.
- [38] S.G. Johnson, J.D. Joannopoulos, Block-iterative frequency-domain methods for Maxwell's equations in a planewave basis, *Opt. Express* 8 (2001) 173–190.
- [39] A. Taflove, et al., *Computational Electrodynamics: The Finite-Difference Time-Domain Method*, Artech House Publishers, 2000.
- [40] M. Notomi, A. Shinya, S. Mitsugi, E. Kuramochi, H.-Y. Ryu, Waveguides, resonators and their coupled elements in photonic crystal slabs, *Opt. Express* 12 (2004) 1551–1561.

Biographies

Xiaodong Yang was born in 1977, and received the MSc degree in physics from the Chinese Academy of Sciences, China, in 2003. He is now a PhD student in Optical Nanostructures Laboratory at Columbia University. His research interests have focused on photonic crystals and silicon photonics.

Chee Wei Wong joined the Columbia Faculty in 2004, after receiving his ScD in mechanical engineering (optical nanotechnology) at the Massachusetts Institute of Technology (MIT) in 2003. He received the SM at MIT in 2001, the BSc in mechanical engineering (highest honors) at the University of California at Berkeley in 1999, and BA in economics (highest honors) at the University of California at Berkeley in 1999. He was a post-doctoral research associate at the MIT Microphotonics Center prior to joining Columbia. His research interests are in optical nanostructures, such as nonlinearities in nanophotonics, quantum dot interactions, high-density integrated optics, silicon electronic-photonics integration, nanoelectromechanical systems, and nanofabrication. He is a member of APS, ASME, IEEE, OSA, and Sigma Xi.